Electronic Supplementary Material (ESI) for Journal of Materials Chemistry A.
This journal is © The Royal Society of Chemistry 2018

Supporting information:

# $H_xMoO_{3-y}$ Nanobelts: An Excellent Alternative to Carbon Electrode for High Performance Mesoscopic Perovskite Solar Cells

*Hua Zhang,[a+] Huan Wang,[b+] Yinglong Yang,[a] Chen Hu,[a] Yang Bai,[a] Teng Zhang,[a] Wei Chen,[b,d] and Shihe Yang [a,c*]*

Dr. H. Zhang, Y. Yang, C. Hu, Dr. Y. Bai, Dr. T. Zhang and Prof. S. Yang
[a]Department of Chemistry, The Hong Kong University of Science and Technology, Clear Water Bay, Kowloon, Hong Kong, China

Dr. H. Wang and Prof. W. Chen
[b]Shenzhen Key Laboratory of Nanobiomechanics, Shenzhen Institutes of Advanced Technology, Chinese Academy of Sciences, Shenzhen, Guangdong 518055, China

Prof. S. Yang
[c]Guangdong Key Lab of Nano-Micro Material Research, School of Chemical Biology and Biotechnology, Shenzhen Graduate School, Peking University, Shenzhen 518055, China

Prof. W. Chen
[d]Wuhan National Laboratory for Optoelectronics, Huazhong University of Science and Technology, Luoyu Road 1037, Wuhan, 430074, China

[+]These authors contribute equally to this work

[*]Corresponding authors. E-mail: chsyang@ust.hk

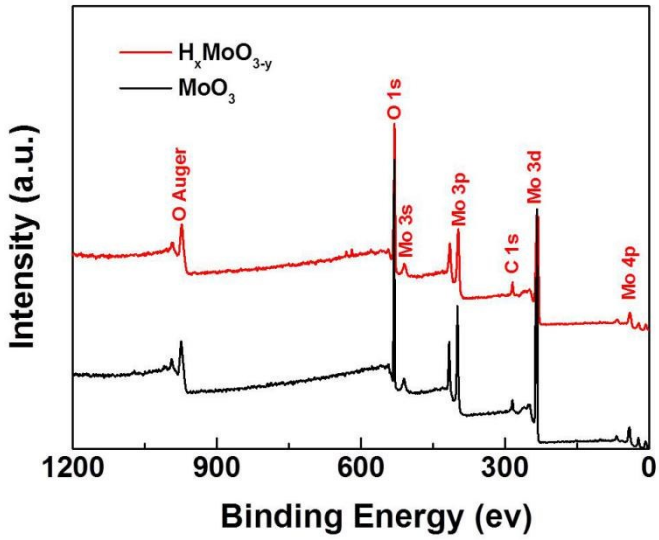


**Figure S1** XPS survey spectra of the α-$MoO_3$ and $H_xMoO_{3-y}$ films.

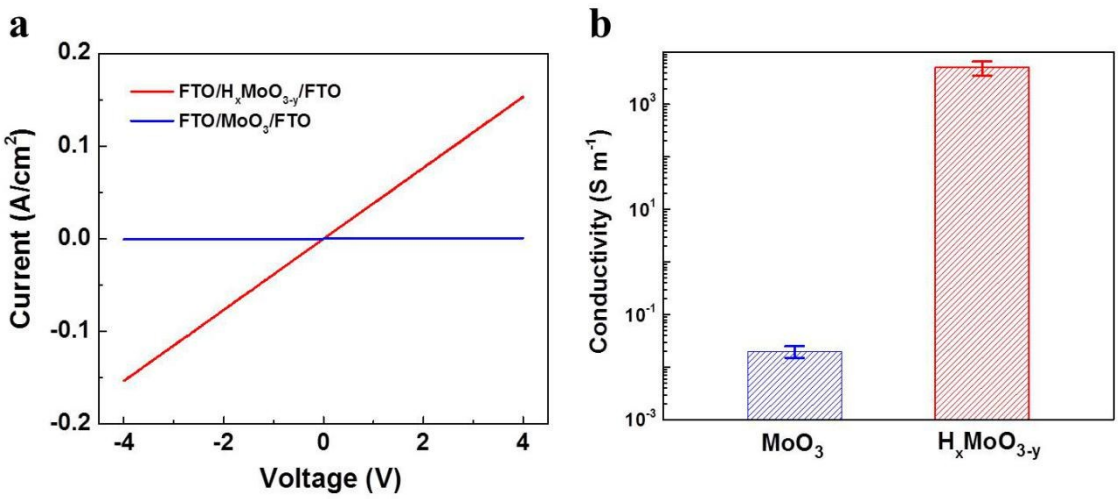


**Figure S2** (a) J-V curves of the α-$MoO_3$ and $H_xMoO_{3-y}$ films with identical thickness. (b) Histogram of specific conductivities based on the α-$MoO_3$ and $H_xMoO_{3-y}$ films, respectively.

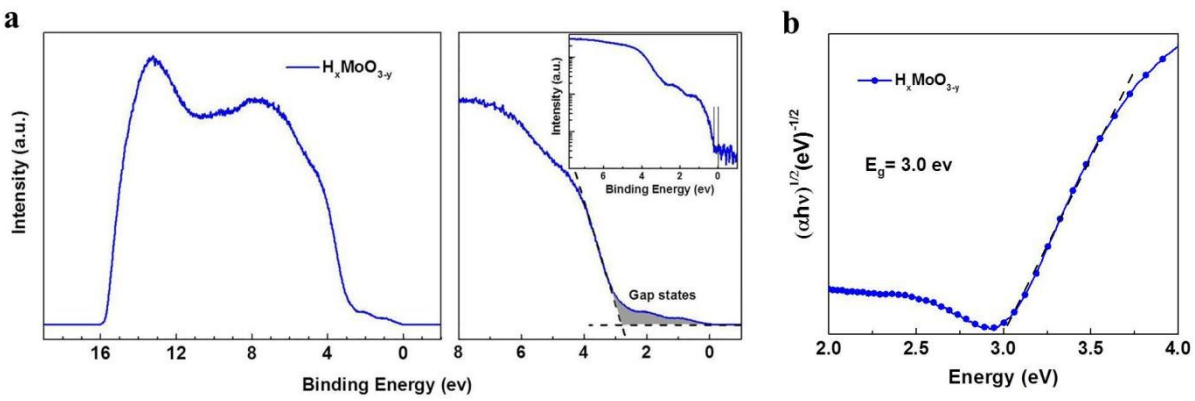


**Figure S3** (**a**) UPS spectra in different energy regions illustrating the derivation of the work function and the top of occupied states. Inset shows the semi-log representation of the valence band region close to the Fermi level. (**b**) The corresponding Tauc plot of the absorbance spectrum.

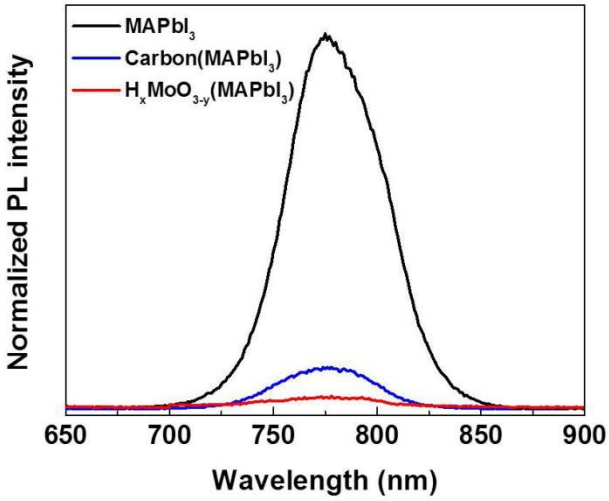


**Figure S4** The steady-state PL spectra of the perovskite filled in the $H_xMoO_{3-y}$ and high-temperature carbon films.

**Table S1.** PL decay curves of the Glass/$MAPbI_3$, Glass/Carbon ($MAPbI_3$), and Glass/ $H_xMoO_{3-y}$ ($MAPbI_3$) samples fitted by a bi-exponential function $I(t)= A_1exp(-t/\tau_1) + A_2exp(-t/\tau_2)$, and $\tau_{avg} = \tau_1 \times (A_1/A_1+A_2) + \tau_2 \times (A_2/A_1+A_2)$.

| Substrates | $A_1/A_1+A_2$ | $\tau_1$ (ns) | $A_2/A_1+A_2$ | $\tau_2$ (ns) | $\tau_{avg}$ (ns) |
|---|---|---|---|---|---|
| **$MAPbI_3$** | 0.48 | 5.43 | 0.53 | 100.04 | 55.63 |
| **Carbon ($MAPbI_3$)** | 0.84 | 9.58 | 0.16 | 12.40 | 10.03 |
| **$H_xMoO_{3-y}$ ($MAPbI_3$)** | 0.71 | 4.36 | 0.29 | 5.02 | 4.55 |

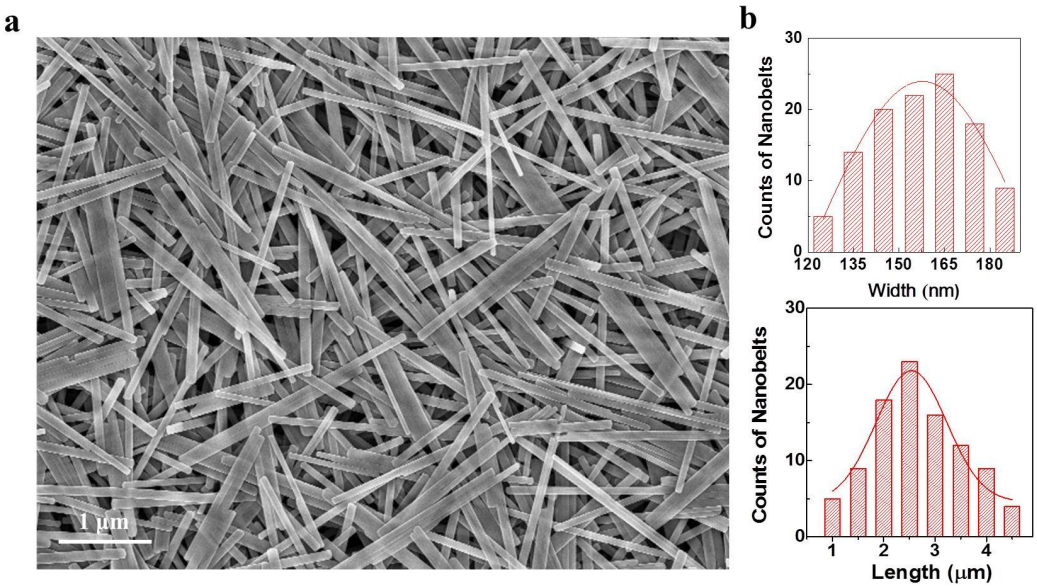


**Figure S5** (**a**) Top view SEM images of $H_xMoO_{3-y}$ film prepared by drop-casting. (**b**) Histogram of the width of $H_xMoO_{3-y}$ nanobelts. (**c**) Histogram of the length of $H_xMoO_{3-y}$ nanobelts.

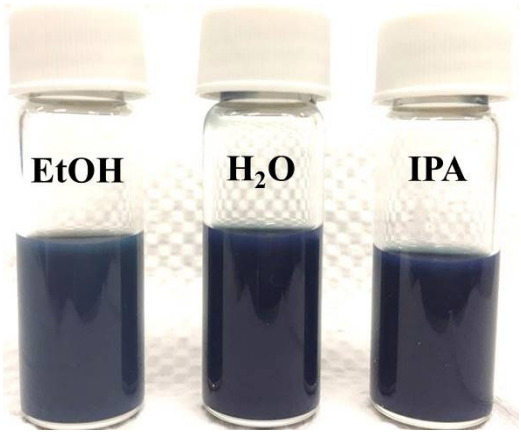


**Figure S6** The optical photographs of highly dispersed $H_xMoO_{3-y}$ solution using deionized water ($H_2O$), ethanol (EtOH) and isopropanol (IPA) solvents, respectively.

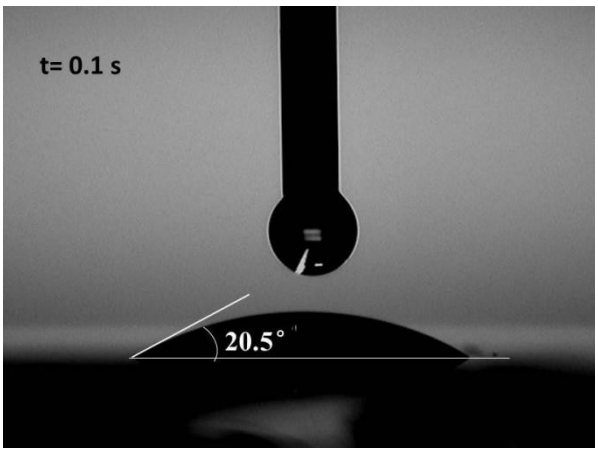


**Figure S7** The contact angle of the $H_xMoO_{3-y}$ film against DMF solvent.

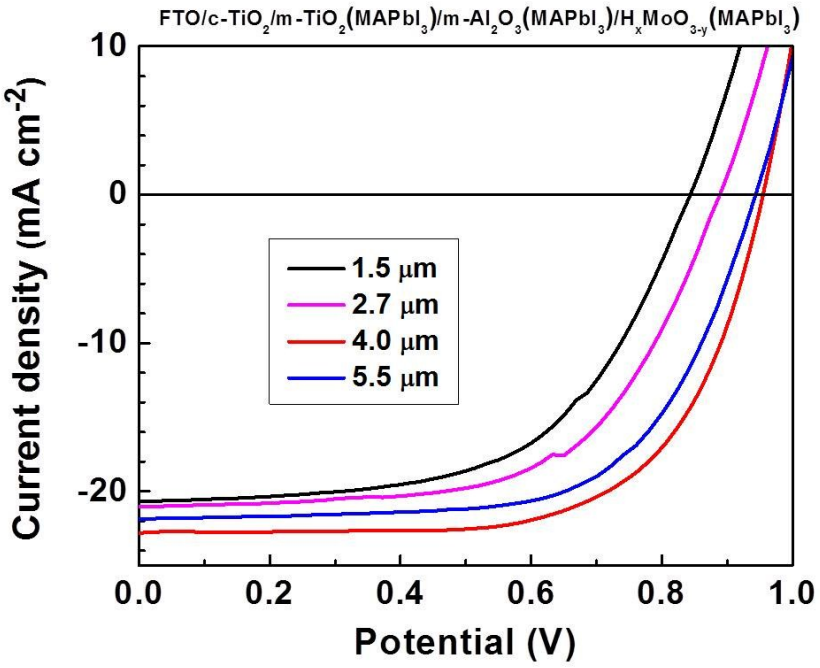


**Figure S8** Thickness dependence of device performance based on the $H_xMoO_{3-y}$ electrode.

**Table S2** Performance summary of the champion devices with different thicknesses of the $H_xMoO_{3-y}$ electrode based on the structure of FTO/c-$TiO_2$/m-$TiO_2$/ m-$Al_2O_3$/$H_xMoO_{3-y}$.

| **Thickness** ( μ m) | $V_{OC}$ (V) | $J_{SC}$ (mA/cm$^2$) | **FF** | **PCE** (%) | $R_{sh}$ ( Ω /cm$^2$) | $R_s$ (Ω/cm$^2$) |
|---|---|---|---|---|---|---|
| **1.5** | 0.84 | 20.81 | 0.58 | 10.1 | 0.6k | 7.5 |
| **2.7** | 0.89 | 21.04 | 0.61 | 11.4 | 2.0k | 6.1 |
| **4.0** | 0.96 | 22.54 | 0.67 | 14.5 | 3.5k | 5.3 |
| **5.5** | 0.95 | 21.90 | 0.64 | 13.3 | 2.8k | 5.8 |

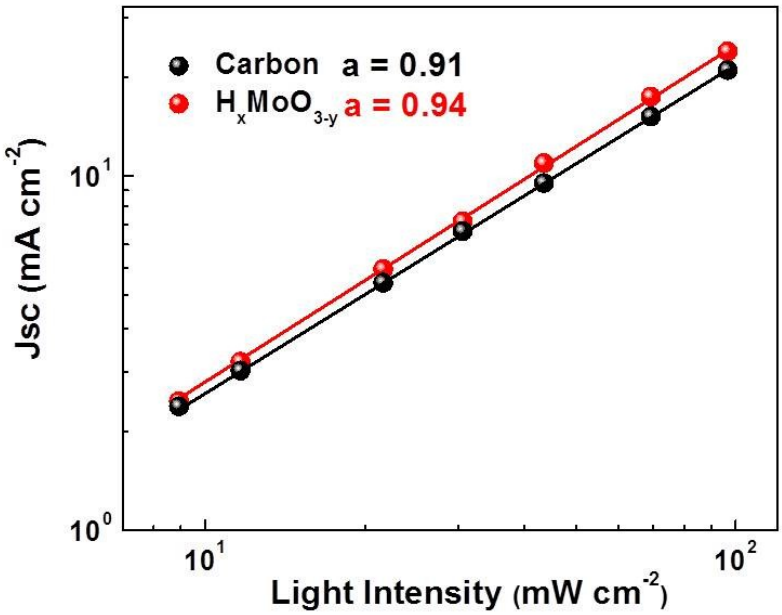


**Figure S9** The light-intensity dependence of $J_{SC}$ for the champion devices based on the high temperature carbon and $H_xMoO_{3-y}$ electrodes, respectively.

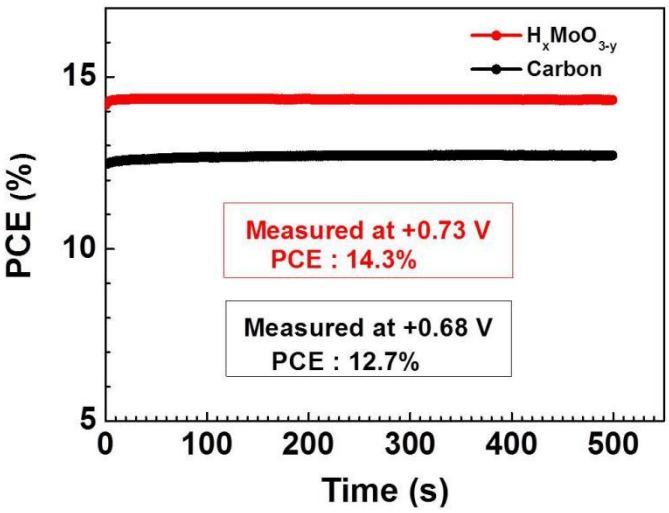


**Figure S10** The steady-state power output at the maximum power point for both the champion devices.

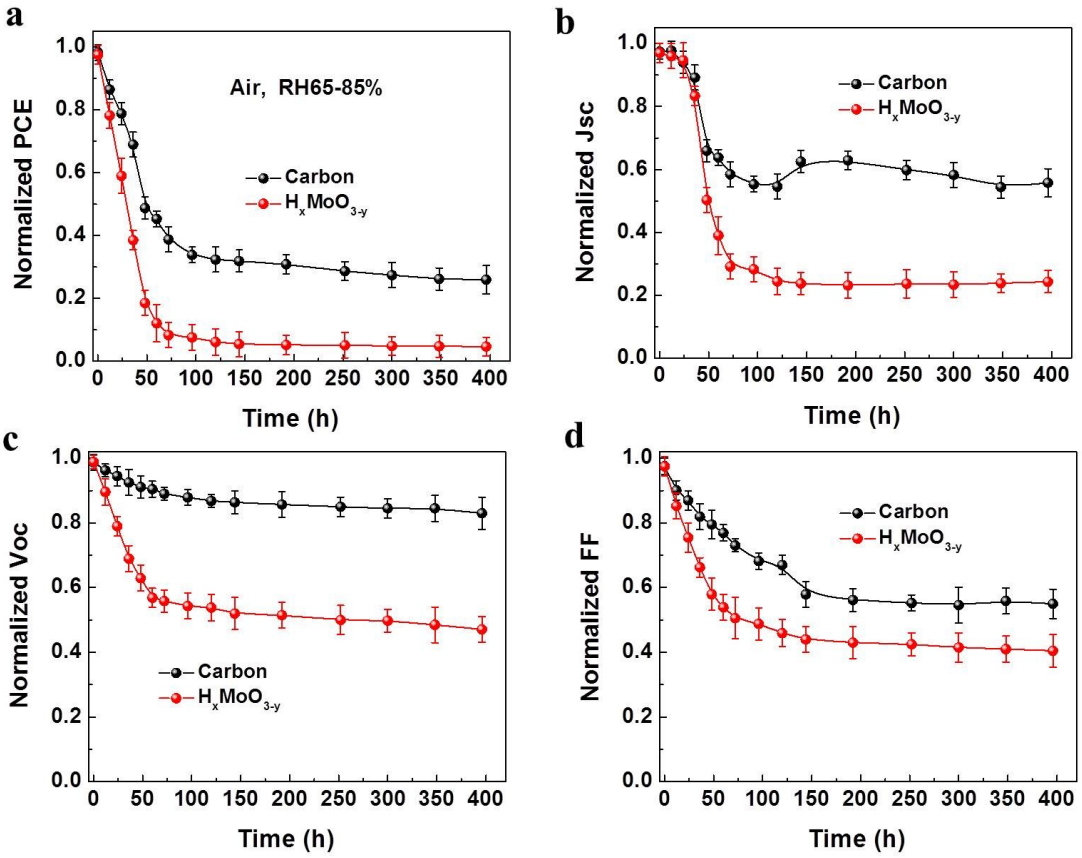


**Figure S11 (a)-(d)** Time-dependent normalized photovoltaic parameters of unsealed devices based on the respective $H_xMoO_{3-y}$ and high temperature carbon electrodes under ambient air at 65-85% relative humidity in the dark.

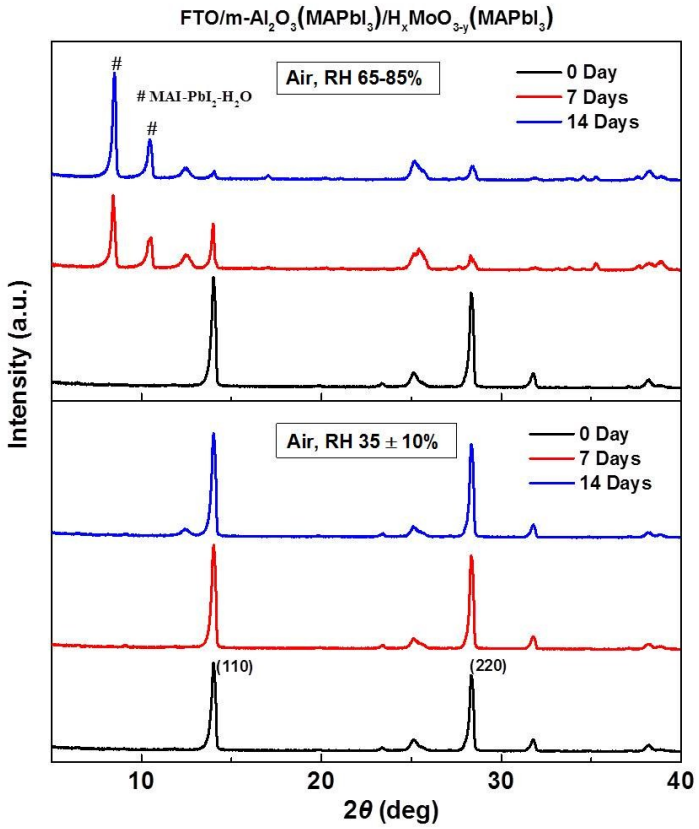


**Figure S12** XRD patterns of the perovskite filled in the structure of FTO/m-$Al_2O_3$/$H_xMoO_{3-y}$ before and after degradation, which were measured after continuously exposing the samples in ambient air at different relative humidity.